Implications of Non-LTE Buffer Gas Effects on ICF Target Chamber Design

J.J. MacFarlane, P. Wang, and G.A. Moses

October 1990

UWFDM-831

Presented at the 9th Topical Meeting on the Technology of Fusion Energy, 7–11 October 1990, Oak Brook IL; Fusion Tech. 19 (1990) 703.

FUSION TECHNOLOGY INSTITUTE

UNIVERSITY OF WISCONSIN

MADISON WISCONSIN

Implications of Non-LTE Buffer Gas Effects on ICF Target Chamber Design

J.J. MacFarlane, P. Wang, and G.A. Moses

Fusion Technology Institute
University of Wisconsin
1500 Engineering Drive
Madison, WI 53706

http://fti.neep.wisc.edu

October 1990

UWFDM-831

Presented at the 9th Topical Meeting on the Technology of Fusion Energy, 7–11 October 1990, Oak Brook IL; Fusion Tech. 19 (1990) 703.

IMPLICATIONS OF NON-LTE BUFFER GAS EFFECTS FOR ICF TARGET CHAMBER DESIGN

J. J. MacFarlane, P. Wang, and G. A. Moses
Fusion Technology Institute
University of Wisconsin-Madison
1500 Johnson Drive
Madison WI 53706
(608) 263-8485

ABSTRACT

We present results from radiation transport calculations for plasma conditions that are expected for the buffer gases of high-gain inertial confinement fusion (ICF) target chambers. In our calculations, the plasmas are *not* assumed to be in local thermodynamic equilibrium (LTE). The state of the plasmas is obtained by solving multilevel atomic rate equations self-consistently with the radiation field. Radiation is transported using an escape probability model. Atomic physics data is generated using a combination of Hartree-Fock, distorted wave, and semi-classical impact parameter models. Our results show that the self-attenuation of line radiation results in a significant reduction in the radiation flux at the target chamber first wall. We compare our results with those from other calculations and find that the heat fluxes at the first wall are significantly lower than previously predicted by multigroup radiation diffusion models. The lower heat fluxes suggest that thermal conduction within the first wall can act to keep temperatures near the surface of the wall much lower than previously thought, thus reducing problems associated with thermal stresses and vaporization. We discuss the ramifications of our results for the SIRIUS-T ICF reactor.

INTRODUCTION

High-gain inertial confinement fusion targets are expected to release roughly 10^7 to 10^9 joules of energy over a very short time period (~10^{-8} seconds). Roughly two-thirds of the energy is carried away by neutrons and is deposited in the "blanket" around the periphery of the target chamber. Most of the remaining energy is emitted in the form of x-rays and high-velocity ions (the target debris). The x-rays and debris ions have rather short mean free paths and deposit their energy within the relatively small amount of material: the target chamber buffer gas and the first several microns of the chamber wall. Energy absorbed by the buffer gas results in the formation of a high temperature "microfireball," which reradiates a significant fraction of its energy to the first wall. In addition, the microfireball rapidly expands and can generate a strong shock (see Figure 1).

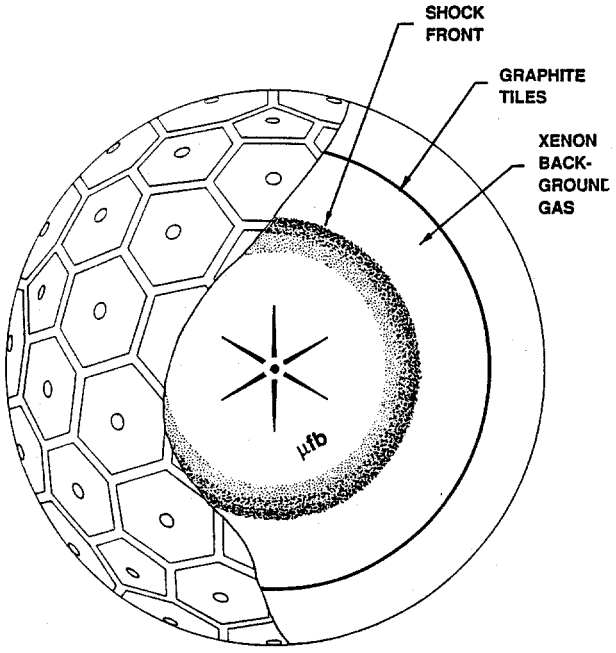

Figure 1. Schematic illustration of the SIRIUS-T target chamber.

A major concern in designing ICF power reactors[1-5] and nearer-term test facilities, such as the Laboratory Microfusion Facility,[6-11] is the protection of the target chamber first wall from the target x-rays and debris ions. For an exposed solid surface, a thin layer ~10 μm thick can absorb a large fraction of this energy, resulting in a significant increase in temperature for the region. Rapid deposition of large amounts of energy in such a small volume can lead to several problems. Large temperature gradients can produce unacceptably large thermal stresses which can cause the first wall material to fail. In addition, high temperatures can cause a thin layer of the first wall (with a mass of ~1 kg) to vaporize. Vaporization in ICF target chambers can be a serious problem because: (1) erosion rates can be excessive, (2) the recoil impulses produced as vapor expands away from the wall can cause structural damage, and (3) the time it takes for vaporized material to recondense or be pumped from the chamber can limit the shot rate for a reactor.[1-3,11]

A variety of techniques have been proposed to protect the target chamber wall. The simplest approach is to fill the target chamber with a moderate density (~1 torr at 0°C) background gas. The purpose of the buffer gas is to stop a large fraction of the x-ray and debris ion energy, and re-release the energy over a relatively long period of time. Using this approach, the time interval over which the energy is deposited at the chamber wall can be increased several orders of magnitude. A second method of protecting the chamber wall is to surround the target with a "debris shield". Harrach[9] and Tabak[10] have suggested that surrounding the target with ~1 kg of plastic or frozen nitrogen. Alternative methods of first wall protection include spraying an array of liquid Li jets about the target,[5] or inserting an array of INPORT tubes filled with liquid LiPb.[2,3] In the latter approaches, the chamber wall is also protected from neutron damage.

The purpose of this paper is to show that buffer gases may offer substantially more protection to the first wall than previously thought. The reason is that a significant fraction of the line radiation emitted by the buffer gas is attenuated before reaching the wall. Line radiation is particularly important at the densities and temperatures expected for target chamber gases because it dominates the exchange of energy between the radiation field and the plasma. The lower fluxes computed with our non-LTE radiative transfer model suggest that the surface temperature of the wall, which is determined by the competition between the radiative flux into the wall and the thermal conductive flux through the wall, may be substantially less than previously predicted.[12]

Below, we present a brief overview of the radiative transfer, ionization, and atomic physics models used for our calculations. We will then present results for simple plasmas at conditions selected from the SIRIUS-T reactor study.[1,12] In particular, we will focus attention on the radiative heat flux escaping the plasma and how it affects the first wall. We also compare our calculated fluxes with those determined from a multigroup radiation diffusion calculation.

THEORETICAL MODELS

Target chamber plasmas created after a high-gain ICF target explosion are very far from local thermodynamic equilibrium. The atomic level populations are *not* well-described by the Saha equation and Boltzmann statistics. The internal energy and opacity at each point in the plasma depend not only on the local temperature and density, but also the radiation field. Also, the radiation flux escaping the plasma is nothing close to that of a blackbody. Target chamber plasmas can be optically thick at some frequencies (e.g., at line centers), while being optically thin in other parts of the spectrum. To better understand these effects, we have developed a non-LTE radiative transfer code[13] and several atomic physics codes.[14] Below, we present a brief overview of the models employed.

Radiation Transport and Ionization Models

A collisional-radiative equilibrium (CRE) model is used to compute the ionization and excitation populations. In this model, the density of atoms (or ions) in level **i**, $\mathbf{n_i}$, is obtained by solving a matrix of steady-state rate equations:

$$\frac{dn_i}{dt} = \sum_j n_j (C_{ji} + R_{ji}) - n_i \sum_j (C_{ij} + R_{ij}) \qquad (1)$$

where $\mathbf{C_{ji}}$ and $\mathbf{R_{ji}}$ are the collisional and radiative transition rates, respectively, from state **j** to **i**. The rates we consider in our model are: collisional excitation and deexcitation, spontaneous decay, photoexcitation and stimulated emission, collisional ionization and recombination, radiative recombination, dielectronic recombination, and photoionization and stimulated recombination. The major difficulty in solving problems of this type is that the photoexcitation and photoionization rates depend on the radiation field. The radiation field in turn depends on the state (i.e., the opacity) of the plasma. Thus, to properly model target chamber plasmas, the atomic rate equations and radiation field must be solved self-consistently.

To model the transport of radiation in target chamber plasmas, we use an escape probability technique.[15,16] Frequency-averaged escape probabilities for bound-bound (line) photons and bound-free photons are calculated using empirical fits to exact numerical results. Angle-averaged zone-to-zone "coupling coefficients" are calculated to determine the photoexcitation and photoionization rates. This model has previously been shown to be computationally efficient and reasonably accurate.[15,16] Because the model requires relatively little computer time (compared to many other non-LTE radiative transfer codes), it can be coupled with hydrodynamics codes to provide a powerful computational tool for simulating rapidly changing plasma, such as target chamber plasmas.

Atomic Physics Data

In our radiative transport model, all levels of an ionization stage are coupled to the ground state of the next higher ionization stage by collisional ionization, photoionization and stimulated recombination, and collisional and radiative recombination. The adjacent ground states are also coupled by dielectronic recombination. The excited levels of a given ion are coupled to other excited levels and the ground state by electron collisional excitation and deexcitation, stimulated absorption and emission, and radiative decay.

In the calculations of atomic energy levels, the interaction between atomic electrons is approximated by an LS-coupling scheme. The energies of the levels and the transition oscillator strengths are generated from Hartree-Fock calculations. The electron collisional excitation rate coefficients employed in this calculation are obtained by two methods. For all electric dipole allowed transitions,

the excitation cross sections are calculated by using the semiclassical impact-parameter method.[17] By comparing with available experimental data and other calculated results, we expect that our excitation cross sections are accurate to about a factor of 2. The rate coefficients are obtained by averaging the cross sections over a Maxwellian electron velocity distribution. The principle of detailed balance is applied to obtain the deexcitation rate coefficients from the excitation rate coefficients.

Electron collisional ionization rate coefficients are calculated using a semi-empirical model,[18] while the electron collisional recombination rate coefficient is obtained by using the principle of detailed balance. Radiative recombination cross sections are obtained from Milne's relation.[19] Photoionization cross sections are generated by using the Hartree-Fock model. Comparison with experimental data[20] shows that Hartree-Fock results are much more accurate than the hydrogenic cross sections. The radiative recombination cross sections are used with the Maxwellian electron distribution to obtain the rate coefficient for radiative recombination to each atomic level. Dielectronic recombination rate coefficients are calculated by using the Burgess-Mertz model.[21]

RESULTS

When a high-gain ICF target explodes within a moderate density (**n** ~10^{16} - 10^{18} cm^{-3}) buffer gas, a significant fraction of the x-ray and debris ion energy is absorbed before it reaches the wall. The gas is rapidly heated and becomes partially ionized. Temperatures within the plasma typically range from less than 1 eV (1 eV = 11,606 K) near the wall of the target chamber to as high as 10^3 eV near the point of explosion. Large pressure gradients cause the plasma to rapidly expand outward, forming a strong shock. Plasma temperatures drop during this time due to both expansive cooling and radiative losses. It is crucial to have a good understanding of the radiative heat flow through the plasma at this time because radiation losses affect both the strength of the shock and the heating of the first wall.

An example of the temperature evolution within a target chamber buffer gas is shown in Figure 2, where the plasma temperature is plotted as a function of distance from the target explosion at several times after the explosion occurs. These numerical simulations were performed for the SIRIUS-T design study[1,12] using the CONRAD radiation-hydrodynamics code[22] and IONMIX equation of state and opacity code.[23] In the SIRIUS-T design, targets explode in a graphite-lined spherical chamber with a radius of 4 meters. The energy released during each explosion is 100 MJ and the chamber is filled with a 1 torr (**n** = 3.5×10^{16} cm^{-3}) xenon buffer gas. About 95% of the 28 MJ released in the form of x-rays and debris ions is stopped in the buffer gas. Figure 2 shows that at 0.3 μs the microfireball has a radius of about 75 cm and a temperature of about 30 eV. A second front ahead of the microfireball is visible at times less than 10 μs. This front forms as the

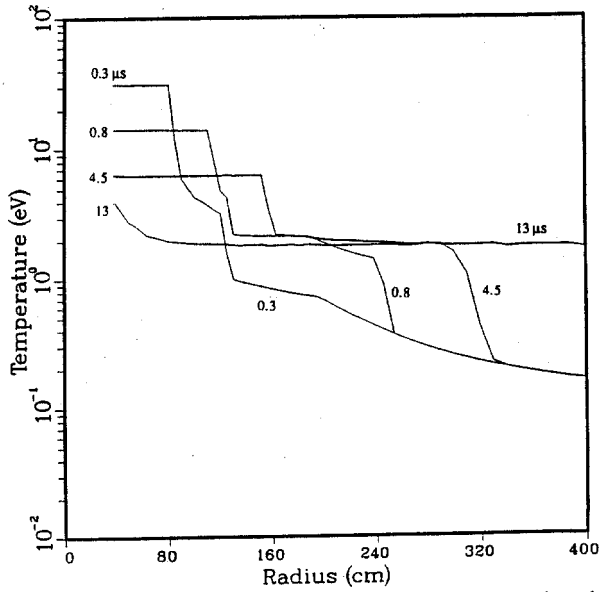

Figure 2. Temperature in the SIRIUS-T target chamber buffer gas vs. distance from the point of explosion. Curves are labelled by the time after explosion (in μs).

debris ions speed through the buffer gas, heating the gas to about 2 eV. The debris ions are completely stopped in the gas by about 1 μs after the target explosion and within a radius of 2.5 meters. The remainder of the gas near the wall is heated as a radiation front propagates outward toward the wall.

At about 12 μs, the radiation front reaches the wall. According to the CONRAD simulations, the radiation heat flux on the wall peaks at this time with a maximum flux of 1.2×10^6 W/cm^2. During the next few microseconds, the temperature at the surface of the graphite tiles — i.e., the first several microns of graphite exposed to the plasma — rises about 1400 K.[12] It is during this time that thermal stresses in the graphite tiles become very large. However, within a few tens of microseconds, the temperature of the surface falls as energy flows through the tiles via thermal conduction.

To gain a better understanding of the radiative properties of target chamber plasmas at the time when the potentially damaging heat flux is highest, we have performed a detailed non-LTE radiation transport calculation using approximately the plasma conditions predicted by CONRAD at 13 μs. Specifically, we have computed the radiative properties for a spherical 4 meter radius plasma, a uniform temperature of 2 eV, and a uniform density of 3×10^{16} cm^{-3}. We have chosen to use neon as the buffer gas instead of xenon because of the relative complexity of the atomic physics associated with the lower ionizations stages of xenon. The conclusions of this paper, however, are unaffected by this choice of buffer gas. For the calculations discussed below, the atomic level structure consists of a modest number of atomic levels (13 levels) distributed over the lowest 3 ionization stages of neon.

Table 1. Radiation Fluxes at the Plasma Boundary (units of ergs/cm^2/s)

Case	Bound-Bound	Bound-Free	Free-Free	Total
Optically Thick	5.2×10^8	1.7×10^{10}	3.0×10^{10}	4.7×10^{10}
Optically Thin	4.0×10^{11}	1.0×10^{11}	2.5×10^{10}	5.3×10^{11}
20 Group Diffusion				3.4×10^{11}
Blackbody				1.7×10^{13}

Figure 3 shows the radiative flux escaping at the boundary of the spherical plasma as a function of photon energy. Several very strong emissions are visible. (In an actual plasma, many more lines would appear. In this calculation, we have considered a rather modest number of levels in our atomic model.) Above the recombination edge at 20 eV the continuum is dominated by bound-free emission, while at lower photon energies, free-free (Bremsstrahlung) emission dominates the continuum. Also shown in Figure 3 is the flux emitted by a blackbody with a temperature of 2 eV. It is obvious that the actual spectrum is not at all well approximated by a blackbody spectrum.

The contribution to the total (frequency-integrated) flux is shown in Table 1. The fluxes in which radiative transfer effects are included are indicated in the row labelled "optically thick." Note that the lines represent only about 1% of the total flux escaping the plasma. For comparison, we performed calculations for a similar case in which attenuation effects — which influence both the atomic level populations and the flux — were ignored ("optically thin" case). In this case, the total flux is about a factor of 7 higher. Also, the line flux contributes to about 75% of the total flux. Relative to the "thin" case, the optically thick line flux is about 3 orders of magnitude lower. This results from the fact that the absorption cross sections are high at the frequencies where the emissivity is also high. Thus, this self-attenuation of line radiation in target chamber plasmas can dramatically reduce the radiative heat flux at the chamber wall.

A major reason for the difficulty of accurately computing the properties of target chamber plasmas is that the photon mean free paths are extremely small at some frequencies, while being quite large (in fact, larger than the chamber radius) at others. Figure 4 shows the optical depth — along a ray from the center of the plasma radially outward to the plasma boundary — as a function of the photon energy. Near the line cores, the optical depth is often quite large; in this case, up to 10^5. On the other hand, at other frequencies the optical depths can be quite small and the photon mean free paths can be much larger than the target chamber. For example, at energies just below the photoionization edge at NeI photoionization edge at 20 eV the optical depth is about 10^{-5}. Because of the wide range of optical depths, computation of the plasma radiative properties requires rather detailed modelling.

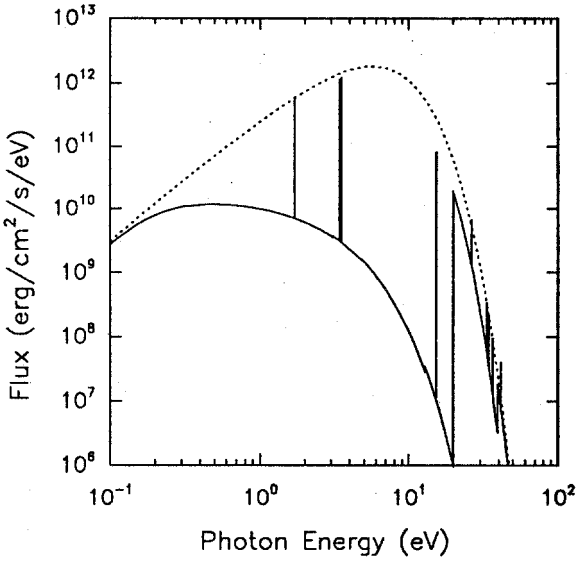

Figure 3. Radiation flux escaping a spherical plasma with T = 2 eV, n = 3×10^{16} cm^{-3}, and R = 4 meters. The dashed curve represents the flux from a blackbody.

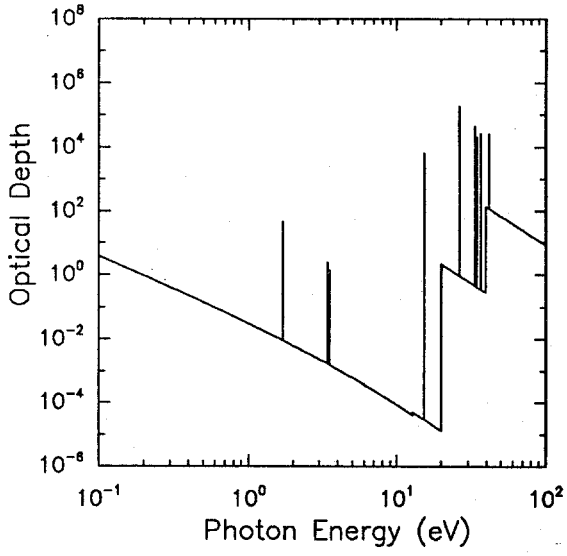

Figure 4. Optical depth from the center of the spherical plasma to the plasma boundary.

We have also compared our results with those obtained using a multigroup radiation diffusion model for a spherical plasma at the same conditions. Diffusion models are often used in radiation-hydrodynamics codes because of their relative ease in programming and computational speed. In the diffusion calculation, 20 groups were used and hydrogenic ion atomic data was supplied by the IONMIX code.[23] A comparison of the spectral fluxes computed using the non-LTE radiative transfer code and the diffusion model is shown in Figure 5. Note that there is considerably more detail in the non-LTE model because lines are transported individually. In addition, the level populations are computed self-consistently with the radiation field. The total flux predicted by the diffusion model is about 36% lower than the optically thin case (see Table 1), but a factor of about 7 - 8 higher than the optically thick case. Also shown in Table 1 is the flux emitted by a blackbody at the same temperature. In short, we find that for typical target chamber plasma conditions, optically thin and 20-group diffusion models can overestimate the flux by about an order of magnitude, while the blackbody flux is about 2 to 3 orders of magnitude too high.

There are several potential sources of error in multigroup diffusion models. For the densities and temperatures of target chamber plasmas, lines are often the dominant contributor to the plasma emissivity and absorption coefficient. These quantities can vary by several orders of magnitude over a very narrow frequency range. This makes the idea of using group-averaged opacities rather suspect because the widths of energy groups are generally orders of magnitude larger than characteristic line widths. In fact, it is found that increasing the number of groups for target chamber simulations can significantly decrease the peak flux.[24] Second, diffusion models are based on the assumption that the photon mean free paths are small compared to the size of the plasma. This assumption does not hold at all photon frequencies for target chamber plasmas. And finally, it has been shown[25] that the radiation field in target chamber plasmas significantly alters the atomic level populations. Thus, opacities depend not only on the local temperature and density, but also on the radiation field.

The lower heat fluxes that result from the self-attenuation of line radiation have important implications for ICF target chamber design. The temperature at the first surface of the target chamber is determined by the competition between the radiative heat flux from the buffer gas and the conductive flux through the first wall. When the radiative flux is reduced, both the temperature and temperature gradients are reduced. Thus, the attenuated fluxes may substantially mitigate some of the problems associated with vaporization and thermal stresses for the first wall. The same conclusions also apply to the use of buffer gases to protect ICF driver components and diagnostic equipment.

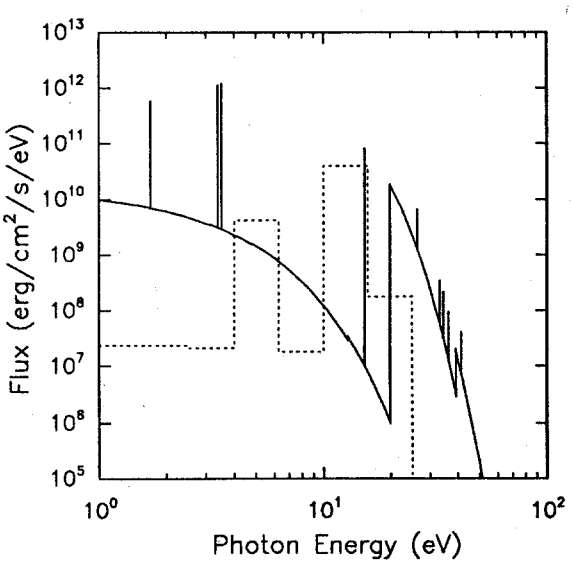

Figure 5. Comparison of fluxes computed using our non-LTE radiative transfer model (solid curve) and a multigroup diffusion model (dotted curve).

CONCLUSIONS

We have presented results from non-LTE radiation transport calculations for plasma conditions that are expected for high-gain ICF target chambers. Our results indicate that line radiation — which is the primary source of energy exchange between the plasma and radiation field — is dramatically attenuated before escaping the target chamber plasma. Comparison with previous calculations indicates that multigroup radiation diffusion models can significantly overestimate the radiation flux at the chamber wall. Our calculations suggest that dry wall reactors may have fewer problems associated with high radiative heat fluxes (e.g., large thermal stresses and vaporization) than previously suspected.

ACKNOWLEDGEMENTS

Support for this work has been provided in part by Kernforschungszentrum Karlsruhe through Fusion Power Associates and Sandia National Laboratories. Computing support has been provided by the National Science Foundation through the San Diego Supercomputing Center.

REFERENCES

1. I.N. SVIATOSLAVSKY, M.E. SAWAN, G.A. MOSES, G.L. KULCINSKI, R.L. ENGELSTAD, E. LARSEN, E. LOVELL, J.J. MacFARLANE, R.R. PETERSON, and L.J. WITTENBERG, "SIRIUS-T, A Symmetric Illumination Tritium Production Facility," Proc. of the 13th Symposium of Fusion Engineering, Knoxville, TN, p. 1416 (1990).

2. G.A. MOSES et al., "Overview of the LIBRA Light Ion Beam Fusion Conceptual Design," Fusion Technology, 15, 756 (1989).

3. B. BADGER et al., "HIBALL — A Conceptual Heavy Ion Beam Driven Fusion Reactor Study," UWFDM-450, University of Wisconsin Fusion Technology Institute Report (1981).

4. J.H. PITTS and I. MAYA, "The CASCADE Inertial Confinement Fusion Power Plant," UCRL-92558, Lawrence Livermore National Laboratory Report (1985).

5. J.A. BLINK, W.J. HOGAN, J. HOVINGH, W.R. MEIER, and J.H. PITTS, "The High-Yield Lithium-Injection Fusion-Energy (HYLIFE) Reactor," UCRL-53559, Lawrence Livermore National Laboratory Report (1985).

6. W.J. HOGAN, "Missions and Design Requirements for a Laboratory Microfusion Facility," Fusion Technology, 15, 541 (1989).

7. R.R. PETERSON, R.L. ENGELSTAD, J.W. POWERS, H.Y. KHATER, M.E. SAWAN, E.G. LOVELL, and G.A. MOSES, "An Overview of Target Chamber Design and Analysis for the Light Ion Beam Laboratory Microfusion Facility," UWFDM-819, University of Wisconsin Fusion Technology Institute Report (1990).

8. J.J. MacFARLANE, R.R. PETERSON, and G.A. MOSES, "Analysis of Physical Processes in ICF Target Chambers: Application to the Laboratory Microfusion Facility," Fusion Technology, 15, 557 (1989).

9. R.J. HARRACH, "High Pressure, Energy, and Impulse Loading of the Wall in a 1-GJ Laboratory Microfusion Facility," UCRL-101646, Lawrence Livermore National Laboratory Report (1989).

10. M. TABAK, "A Sacrificial X-ray and Debris Shield for ICF First Wall Protection," Bull. Amer. Phys. Soc., 34, 2144 (1989).

11. R.R. PETERSON, Gas Condensation Phenomena in Inertial Confinement Fusion Reaction Chambers, Laser Interaction and Related Plasma Phenomena, Vol. 7, Eds. H. Hora and G. Miley, Plenum, (1986).

12. J.J. MacFARLANE, G.A. MOSES, R.R. PETERSON, and I.N. SVIATOSLAVSKY, "Energy Deposition and First Wall Response in the SIRIUS-T Target Chamber," Proc. of the 13th Symposium of Fusion Engineering, Knoxville, TN, p. 746 (1990).

13. J.J. MacFARLANE, P. WANG, and G.A. MOSES, "A Model for Computing Radiation Transport in Moderate Density Plasmas," UWFDM-822, University of Wisconsin Fusion Technology Institute Report (1990).

14. P. WANG, Ph.D. Dissertation, University of Wisconsin, in preparation.

15. J.P. APRUZESE, J. DAVIS, D. DUSTON, and K.G. WHITNEY, J. Quant. Spectrosc. Radiat. Transfer, 23, 479 (1980).

16. J.P. APRUZESE, J. Quant. Spectrosc. Radiat. Transfer, 25, 419 (1981).

17. A. BURGESS and H.P. SUMMER, Mon. Not. R. Astr. Soc., 174, 345 (1976).

18. A. BURGESS and M.C. CHIDICHIMO, Mon. Not. R. Astr. Soc., 203, 1269 (1983).

19. I.I. SOBELMAN, L.A. VAINSHTEIN, and E.A. YUKOV, Excitation of Atoms and Broadening of Spectral Lines, Springer-Verlag, New York.(1981)

20. G.V. MARR and J.B. WEST, At. Data Nucl. Data Tables, 18, 497 (1976).

21. D.E. POST, R.V. JENSEN, C.B. TARTER, W.H. GRASBERGER, and W.A. LOKKE, At. Data Nucl. Data Tables, 20, 397 (1977).

22. R.R. PETERSON, J.J. MacFARLANE, and G.A. MOSES, "CONRAD — A Combined Radiation-Hydrodynamics Vaporization-Condensation Computer Code," UWFDM-670, University of Wisconsin Fusion Technology Institute Report (1988).

23. J.J. MacFARLANE, "IONMIX — A Code for Computing the Equation of State and Radiative Properties of LTE and Non-LTE Plasmas," Comput. Phys. Commun., 56, 259 (1989).

24. I.N. SVIATOSLAVSKY, G.L. KULCINSKI, G.A. MOSES, M.E. SAWAN, R.L. ENGELSTAD, E. LARSEN, E. LOVELL, J.J. MacFARLANE, E. MOGAHED, R.R. PETERSON, J.W. POWERS, and L.J. WITTENBERG, "SIRIUS-T, An Advanced Tritium Production Facility Utilizing Symmetrically Illuminated Inertial Confinement Fusion," these proceedings.

25. J.J. MacFARLANE, P. WANG, and G.A. MOSES, "Non-LTE Radiation Transport in Moderate Density Plasmas," submitted to Lasers and Particle Beams (1990).